

# PREPARATION AND PROPERTIES OF ZrB<sub>2</sub>-SiC COMPOSITES BY CENTRIFUGAL GEL CASTING PROCESS

Dongyang Zhang, Ping Hu and Xinghong Zhang

Science and Technology on Advanced Composites in Special Environment Laboratory, Harbin  
Institute of Technology, Harbin 150001, China

\*Corresponding author: zhangdyhit88@163.com (Dongyang Zhang)

**Keywords:** ZrB<sub>2</sub>-SiC; Centrifugal gel casting; Pressureless sintering; Mechanical properties

## ABSTRACT

High-performance ZrB<sub>2</sub>-SiC composites with homogeneous microstructures had been fabricated by centrifugal gel casting and pressureless sintering. The effects of pH value, dispersant and solid loading on the stability and rheological properties of ZrB<sub>2</sub>-SiC slurries were investigated systematically. Well-dispersed ZrB<sub>2</sub>-SiC suspensions with solid loading up to 48 vol.% were achieved when 0.6 wt.% polyacrylic acid (PAA) was added with pH=11, which was favourable for centrifugal gel casting process. After pressureless sintering at 1900 °C for 2 h, ZrB<sub>2</sub>-SiC ceramics exhibited a homogeneous microstructure and an excellent mechanical properties, and the relative density, flexural strength and fracture toughness of such material were 91.2 %, 370 ± 10 MPa and 3.67 ± 0.19 MPa m<sup>1/2</sup>, respectively. This work provide a promising method to fabricate uniform multiphase materials with high packing density.

## 1 INTRODUCTION

ZrB<sub>2</sub>-based ultra-high temperature ceramics (UHTCs) are promising candidates for thermal protection materials in both re-entry and hypersonic vehicles due to many excellent properties, such as high melting point, superior strength, good electric and thermal conductivities [1-4]. These excellent properties make ZrB<sub>2</sub>-based UHTCs attractive for use in extreme environments, such as sharp nosecones, leading edges and propulsion components [5-8].

As with other nonoxide ceramics, ZrB<sub>2</sub> ceramics would oxidize when exposed to air at elevated temperatures. The addition of SiC resulted in a significant decrease in the oxidation rate of ZrB<sub>2</sub> due to the formation of an adherent protective layer of borosilicate glass [9-11]. The ZrB<sub>2</sub>-SiC ceramics were usually densified by hot pressing [12] or spark plasma sintering [13], which limited to obtain samples with simple geometry and moderate sizes, and requires costly and time-consuming electrical machining to obtain complex-shaped components [14]. Recently, the colloidal processing, such as slip casting [15], tape casting [16], centrifugal casting [17] and gelcasting [18], was used to consolidate ceramic components to near-net shape. Among colloidal processing, gelcasting is a potential colloidal processing to achieve green ceramic bodies with high strength and uniform microstructure, because the ceramic particles were coated by in-situ polymerized macromolecular gel networks [19]. In the gelcasting process, the solid loading significantly affected the rheological properties and correlated strongly with the green density of the ceramics. The high solid loading in the slurries produced a green body having the lowest possible shrinkage upon drying and reaching to high density [20]. However, it must be noted that the viscosity of the slurry increased with the increasing of the solid loading, thus the problem of the air bubbles trapped in the suspensions became more critical [21]. Even though a routine deairing step was commonly manipulate to avoid large defects caused by entrapped air bubbles, the result was not sufficiently satisfactory [22-23]. Using high centrifugal acceleration for fabricating highly concentrated slurries was an effective solution for eliminating entrapped air bubbles, however, this technique increased the number of heterogeneities among ceramic particles and slightly detracted from the particle packing and final properties of ceramics [24].

In this paper, we proposed a novel "centrifugal gel casting" method to fabricate high-performance ZrB<sub>2</sub>-SiC ceramics with homogenous microstructure. The dispersion behaviour and rheology properties of ZrB<sub>2</sub>-SiC slurries were analysed in detail, and the microstructure and mechanical properties of pressureless sintered material were also studied.

## 2 EXPERIMENTS PROCEDURE

### 2.1 Raw materials

Commercially available  $ZrB_2$  powders (average particle size  $\sim 2 \mu m$ , purity  $> 99.5\%$ , Beijing HWRK Chem Co. Ltd., China) and SiC powders (average particle size  $\sim 0.5 \mu m$ , purity  $> 99\%$ , Weifang Kaihua SiC Micro-powder Co. Ltd., Weifang, China) were used as raw materials in this study.  $B_4C$  powder ( $1\sim 2 \mu m$ ; Aladdin Industrial Corporation, Shanghai, China) and phenolic resin (55 % remaining carbon; Shengquan Hi-Tech Material Co. Ltd., Yinkou, China) were used as sintering additives. For aqueous centrifugal gel casting purpose, acrylamide (AM,  $C_2H_3CONH_2$ ) and N,N'-methylenebisacrylamide (MBAM,  $(C_2H_3CONH)_2CH_2$ ) were used as monomer and crosslinker, respectively. Ammonium persulfate ( $(NH_4)_2S_2O_8$ , APS) was used as initiator, and the catalyst was N,N,N',N'-tetramethylethylenediamine ( $C_6H_{16}N_2$ , TEMED). To obtain well-dispersed  $ZrB_2$ -SiC slurries, four kinds of dispersants, polyarylic acid, polyethylenimine, ammonium polyacrylate and ammonium citrate were used as dispersant to produce high concentrated suspensions with low viscosity. The pH value was adjusted by hydrochloric acid (HCl) and ammonia water ( $NH_4OH$ ). All of these analytical reagents were chemically pure.

### 2.2 Sample preparation

Fig. 1 presented a flow chart for the overall process of the fabrication of high-performance  $ZrB_2$ -SiC ceramics. Firstly, the monomer and crosslinker was dissolved in the demonized water to obtain the colloidal solutions (Deionized water:AM:MBAM=28:1:0.1), namely the monomer content was 3.5wt.% (based on added deionized water) and the ratio of crosslinker to monomer was 1:10. In addition, pH value of the solutions was adjusted by HCl or  $NH_4OH$ . Then  $ZrB_2$ -20vol.%SiC-4vol.% $B_4C$ -2vol.%C mixed powders with different dispersants were added into the colloidal solutions. To obtain the well-dispersed suspensions, the  $ZrB_2$ -SiC slurries was ball-milled for 10 h at 250 rpm in demonized water using WC as the media. For centrifugal gel casting, the initiator (4 wt.%, based on the monomer content) without any catalyst were added by vigorous mixing and were spun in a PTFE mold for 10 min at a centrifugal speed of 9000r/min in a centrifuge equipped with swinging buckets. After centrifugation, the molds containing slurries were dwelled for 45min for gelation process in water bath of  $70 \text{ }^\circ C$ . The samples were achieved after drying freely in constant temperature ( $25 \text{ }^\circ C$ ) and humidity (98 %) for 2 days and then demolded carefully. For subsequent experiments, the samples were heated to  $800 \text{ }^\circ C$  for 2 h to control the gas release during remove of the polymer. Finally, pressureless sintering was performed at  $1900 \text{ }^\circ C$  for 2 h in an argon atmosphere.

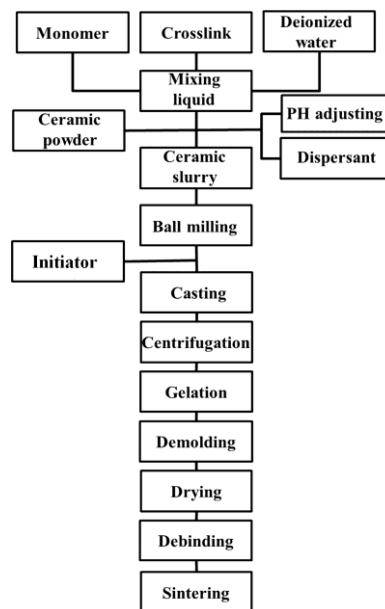


Figure 1: Flow chart of the centrifugal gel casting process

## 2.3 Characterization

The surface charge behavior of ZrB<sub>2</sub> and SiC powders (0.01 vol.% solid loading) as a function of pH with and without dispersant were characterized by a zeta potential analyzer (Malvern Zetasizer Nano ZS, Malvern Instruments Ltd., UK). The average particle size of the ceramic powders was measured by a laser particle size analyzer (Hylology Instruments Co. Ltd., Dandong, China). The sedimentation measurement were carried out by injecting the suspensions into cuvettes and then covering with caps to avoid evaporation. After sedimentation for 3 h, the stabilities of the suspensions were judged by the rate of H to H<sub>0</sub> (H/H<sub>0</sub>), where the H value represented the sedimentation height and the H<sub>0</sub> value represented the original height of the suspensions. Moreover, the viscosity of the aqueous ZrB<sub>2</sub>-20 vol.%SiC suspensions with different solid loading was tested by a viscometer (DV-II+Pro, Brookfield Ltd., USA). The bulk densities of the composites were measured by the Archimedes method with distilled water as the medium. The microstructures of sintered bodies were observed by scanning electron microscopy (SEM, FEI Quanta 200F, USA). The flexural strength ( $\sigma$ ) was measured by three-point bending tests (Model 5569, Instron, USA) with sample size of 3×4×36 mm<sup>3</sup> with a span of 30 mm and a cross-head speed of 0.5 mm min<sup>-1</sup> at room temperature. Fracture toughness (K<sub>IC</sub>) was evaluated by single-edge notched beam (SENB) with tested bars size of 2×4×22 mm<sup>3</sup>, with a notched depth and width of 2 mm and 0.2 mm, respectively, using a span of 16 mm and cross-head speed of 0.05 mm min<sup>-1</sup>.

## 3 RESULTS AND DISCUSSION

### 3.1 Zeta potential measurements of ZrB<sub>2</sub> and SiC particles

Fig. 2 showed the relationship of the Zeta potentials of the ZrB<sub>2</sub> and SiC slurries with the pH values. It can be seen that the zero potential point of ZrB<sub>2</sub> suspensions was achieved when pH value was approached to 6.6, which was closed to the reported value of ZrO<sub>2</sub> slurries [25]. When the pH value was adjusted to 11, the Zeta potential of ZrB<sub>2</sub> and SiC suspensions was approached to -40.8 mV and -50.8 mV, respectively, indicating that the well-dispersed suspensions with good fluidity was achieved. Moreover, the ZrB<sub>2</sub>-SiC suspensions with maximum absolute Zeta potentials was also achieve at pH=11, which was attributed to the improvement of the electrophoresis mobility and dominant electrostatic repulsion. In addition, the particle size distribution of ZrB<sub>2</sub> and SiC powders with different pH value was presented in Fig. 3. The particle size distribution of the powders is a key factor that influences its stability properties [26]. It was obviously noted that the median diameter D50 of ZrB<sub>2</sub> and SiC slurries approached to the minimum when pH value was adjusted to 11 owing to the improvement of the electrostatic repulsion of the double electric layer between the particles. Therefore, the ZrB<sub>2</sub>-SiC suspensions exhibited the optimum dispersion stability under the condition of water dispersion at pH=11.

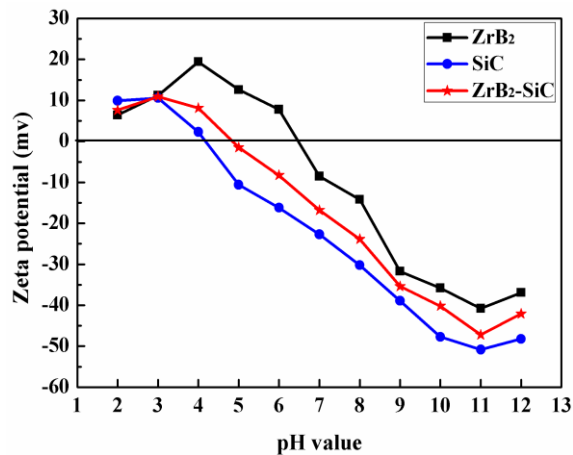


Figure 2: The Zeta potential as a function of pH value

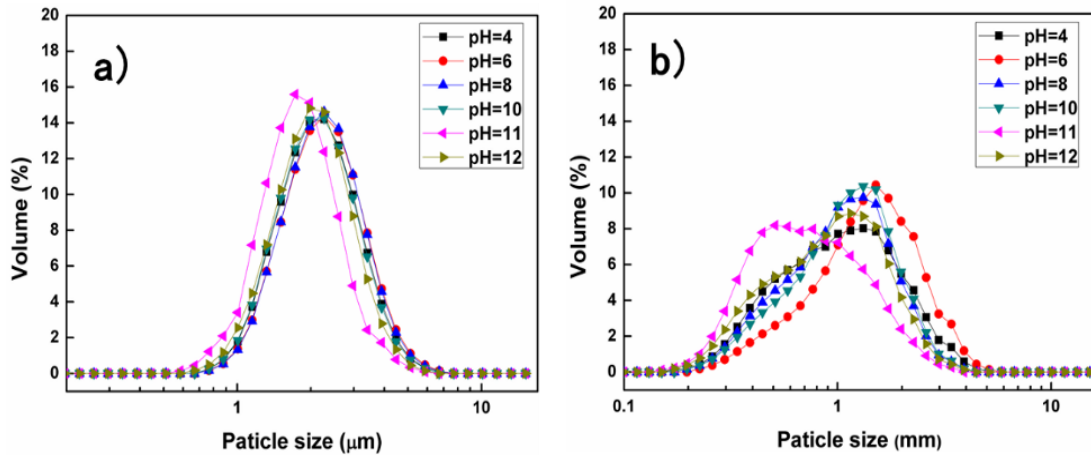


Figure 3: The particle size distribution of powders with different pH value a).  $ZrB_2$  b). SiC

### 3.2 Rheological properties of $ZrB_2$ -SiC suspensions

#### 3.2.1 Effect of dispersant on the rheological properties

In order to investigate the surface adsorbability of different dispersants on the  $ZrB_2$ -SiC suspensions, the sedimentation experiments was conducted to choose the most suitable dispersant, which was showed in Fig. 4. The  $ZrB_2$ -SiC slurries could maintain a mechanical equilibrium state in a short time without settling effect, and the particle in the slurries occurred significant sedimentation effects with the extension of the setting time. It is worthy noted that the settling ratio of  $ZrB_2$ -SiC slurries with PAA dispersant approached to the minimum, indicating that most of the particles were located in a suspended state without settling. The organic acid anion ionized by the anionic PAA dispersant was effectively adsorbed on the surface of the particles to improve the surface electricity, and ultimately achieved the purpose of stable dispersion. Therefore, it was efficient to introduce the PAA dispersant into the slurries to optimize the stability of the  $ZrB_2$ -SiC suspensions.

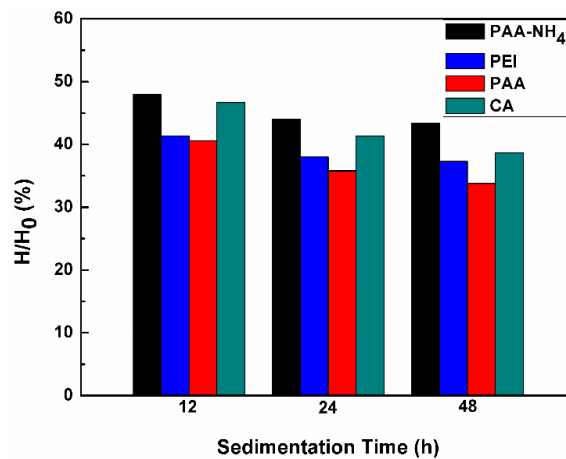


Figure 4: The effect of the dispersant types on the sedimentation volume of  $ZrB_2$ -SiC slurries

Among many factors, the concentration of the dispersant is a vital factor for obtaining optimal aqueous slurries. The optimization of PAA dispersant concentration was carried out by sedimentation experiments, which was presented in Fig. 5. The minimum sedimentation volume of slurry responded to 0.6 wt.% dispersant concentration due to the optimal coverage ratio of dispersant to the particle surface. Neither low concentration nor high concentration had an efficient dispersion effect on the  $ZrB_2$ -SiC suspensions, and the particle was still prone to contact with each other due to insufficient dispersant molecules with low dispersant additive, while there would be a large amount of residual long-link dispersant molecules in the solution to bridge-link and result in gravitation sediment when

the concentration was too high. Hence, it presented that 0.6 wt.% PAA dispersant concentration was optimal to cover particles uniformly and obtain a well-dispersed ZrB<sub>2</sub>-SiC suspensions.

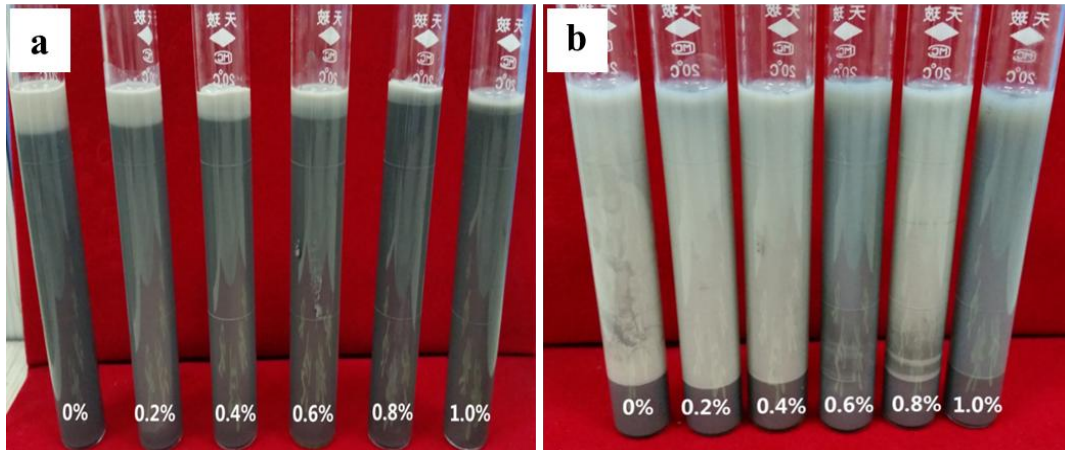


Figure 5: Relationship between the sedimentation volume and the PAA dispersant concentration

### 3.2.2 Effect of the solid loading on the rheological properties

The ZrB<sub>2</sub>-SiC slurries with high solid loading and low viscosity was of crucial importance to the centrifugal gel casting processing, which was directly related to the relative density and the microstructure of green bodies. The viscosity of ZrB<sub>2</sub>-SiC suspensions increased with the increased solid loading according to the Fig. 6. The viscosity of 48 vol.% solid loading suspension was low (1.50 Pa s at 60 S<sup>-1</sup>), which was desirable for the centrifugal gel casting process. When the solid loading increased to 50 vol.%, the movement of the particles was hampered, resulting in the increase of the viscosity. Therefore, the ZrB<sub>2</sub>-SiC suspensions with a solid loading up to 48 vol.% was suitable for centrifugal gel casting and achieving a high green density.

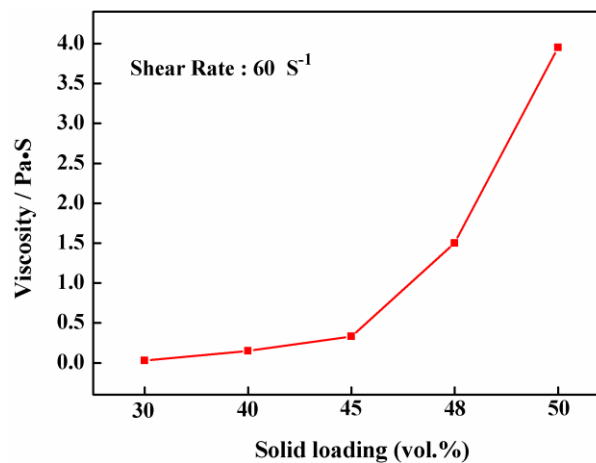


Figure 6: The effect of the solid loading on the viscosity at 60 S<sup>-1</sup> shear rate (0.6 wt.% PAA at pH 11)

### 3.3 Aqueous centrifugal gel casting and pressureless sintering

In the present research, the well-dispersed ZrB<sub>2</sub>-SiC with 48 vol.% solid loading and low viscosity was obtained successfully using 0.6 wt.% PAA dispersant at pH 11. The high-performance ZrB<sub>2</sub>-SiC ceramics were fabricated successfully after aqueous centrifugal gel casting and pressureless sintering at 1900 °C for 2 h. The microstructures of sintered ZrB<sub>2</sub>-SiC pellets were investigated by examining fractured and polished surfaces, which was presented in Fig. 7. The relative density of sintered ZrB<sub>2</sub>-SiC ceramics was 91.8 %, and the flexural strength and fracture toughness were 370 ± 10MPa and 3.67 ± 0.19 MPa m<sup>1/2</sup>, respectively. In addition, the examination of the microstructure after sintering

revealed an average grain size of about 4  $\mu\text{m}$  for  $\text{ZrB}_2$  and about 1  $\mu\text{m}$  for SiC. The dark SiC phase were homogenously dispersed in the  $\text{ZrB}_2$  matrix and no obvious agglomeration was detected.

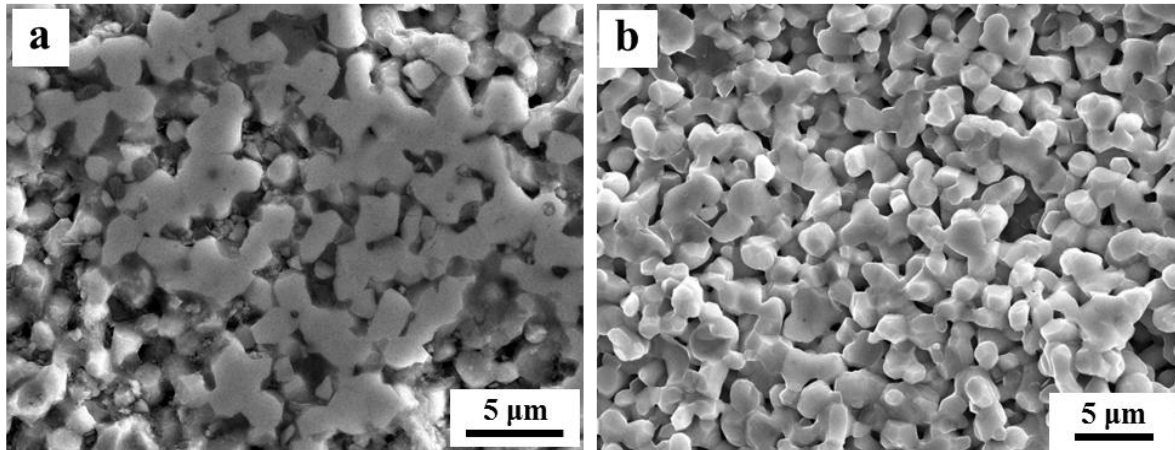


Figure 7: SEM images of pressureless sintered  $\text{ZrB}_2$ -SiC ceramics a. polished surface b. fractured surface

#### 4 CONCLUSIONS

High-performance of  $\text{ZrB}_2$ -SiC composites with uniform microstructures had been successfully fabricated by a novel method called centrifugal gel casting process. Well-dispersed  $\text{ZrB}_2$ -SiC suspensions with solid loading up to 48 vol.% and low viscosity (1.50 Pa s at  $60 \text{ S}^{-1}$ ) was achieved by adding 0.6 wt.% PAA dispersant and adjusting pH value to 11. The crack-free green  $\text{ZrB}_2$ -SiC bodies with 3.5 wt.% monomer was fabricated by centrifugal gel casting process at a centrifugal speed of 9000 r/min for 10 min. Then the dried green bodies were pressureless sintered at 1900  $^\circ\text{C}$  for 2 h to achieve a relative density of 91.8 %, and the average particle size of  $\text{ZrB}_2$  and SiC were 4  $\mu\text{m}$  and 1  $\mu\text{m}$ , respectively. The measured flexural strength and fracture toughness of  $\text{ZrB}_2$ -SiC were  $370 \pm 10 \text{ MPa}$  and  $3.67 \pm 0.19 \text{ MPa m}^{1/2}$ , respectively. This work produced a novel method called centrifugal gel casting, which combined the advantages of gelcasting and centrifugal casting process to fabricate multiphase materials with high packing density and homogenous microstructure.

#### ACKNOWLEDGEMENTS

Financial support was provided by Innovative Research Group of National Nature Science Foundation of China (No. 11421091) and the National Fund for Distinguished Young Scholars (No. 51525201).

#### REFERENCES

- [1]. M. M. Opeka, I. G. Talmy, E. J. Wuchina, J. A. Zaykoskia and S. J. Causeyb, Mechanical, thermal, and oxidation properties of refractory hafnium and zirconium compounds, *Journal of the European Ceramic Society*, **19**, 1999, pp. 2405-2414.
- [2]. A. L. Chamberlain, W. G. Fahrenholtz, G. E. Hilmas and D. T. Ellerby, High-strength zirconium diboride-based ceramics, *Journal of the American Ceramic Society*, **87**, 2004, pp. 1170-1172.
- [3]. S. Q. Guo, Densification of  $\text{ZrB}_2$ -based composites and their mechanical and physical properties: A review, *Journal of the European Ceramic Society*, **29**, 2009, pp. 995-1011.
- [4]. W. G. Fahrenholtz, G. E. Hilmas, I. G. Talmy and J. A. Zaykoski, Refractory diborides of zirconium and hafnium, *Journal of the American Ceramic Society*, **90**, 2007, pp. 1347-1364.
- [5]. N. P. Padture, Advanced structural ceramics in aerospace propulsion, *Nature Materials*, **15**, 2016, pp. 804-809.

- [6]. T. H. Squire, J. Marschall, Material property requirements for analysis and design of UHTC components in hypersonic applications, *Journal of the European Ceramic Society*, **30**, 2010, pp. 2239-2251.
- [7]. T. A. Parthasarathy, M. D. Petry, M. K. Cinibulk, T. Mathur and M. R. Gruber, Thermal and oxidation response of UHTC leading edge samples exposed to simulated hypersonic flight conditions, *Journal of the American Ceramic Society*, **96**, 2013, pp. 907-915.
- [8]. X. Zhang, P. Hu, J. Han and S. Meng, Ablation behavior of ZrB<sub>2</sub>-SiC ultra high temperature ceramics under simulated atmospheric re-entry conditions. *Composite Science and Technology*, **68**, 2008, pp. 1718-1726.
- [9]. W. G. Fahrenholtz, Thermodynamic Analysis of ZrB<sub>2</sub>-SiC oxidation: formation of a SiC-depleted region, *Journal of the American Ceramic Society*, **90**, 2007, pp. 143-148.
- [10]. F. Monteverde and A. Bellosi, Oxidation of ZrB<sub>2</sub>-based ceramics in dry air, *Journal of the Electrochemical Society*, **150**, 2003, pp. 552-559.
- [11]. A. Rezaie, W. G. Fahrenholtz and G. E. Hilmas, Evolution of structure during the oxidation of zirconium diboride-silicon carbide in air up to 1500 °C, *Journal of the European Ceramic Society*, **27**, 2007, pp. 2495-2501.
- [12]. A. Rezaie, W. G. Fahrenholtz and G. E. Hilmas, Effect of hot pressing time and temperature on the microstructure and mechanical properties of ZrB<sub>2</sub>-SiC, *Journal of Materials Science*, **42**, 2007, pp. 2735-2744.
- [13]. I. Akin, M. Hotta, F. C. Sahin, O. Yucela, G. Gollera and T. Gotob, Microstructure and densification of ZrB<sub>2</sub>-SiC composites prepared by spark plasma sintering, *Journal of the European Ceramic Society*, **29**, 2009, pp. 2379-2385.
- [14]. S. Zhu, W. G. Fahrenholtz and G. E. Hilmas, Influence of silicon carbide particle size on the microstructure and mechanical properties of zirconium diboride-silicon carbide ceramics, *Journal of the European Ceramic Society*, **27**, 2007, pp. 2077-2083.
- [15]. V. Medri, C. Capiani and A. Bellosi, Properties of slip-cast and pressureless-sintered ZrB<sub>2</sub>-SiC composites, *International Journal of Applied Ceramic Technology*, **8**, 2011, pp. 351-359.
- [16]. Z. Lü, D. Jiang, J. Zhang and Q. Lin, Aqueous tape casting of zirconium diboride, *Journal of the American Ceramic Society*, **92**, 2009, pp. 2212-2217.
- [17]. W. S. Ebhota, A. S. Karun and F. L. Inambao, Centrifugal casting technique baseline knowledge, applications, and processing parameters: overview, *International Journal of Materials Research*, **107**, 2016, pp. 960-969.
- [18]. R. He, X. Zhang, P. Hu, C. Liu and W. Han, Aqueous gelcasting of ZrB<sub>2</sub>-SiC ultra high temperature ceramics, *Ceramics International*, **38**, 2012, pp. 5411-5418.
- [19]. O. O. Omatete, M. A. Janney and S. D. Nunn, Gelcasting: from laboratory development toward industrial production, *Journal of the European Ceramic Society*, **17**, 1997, pp. 407-413.
- [20]. R. He, P. Hu, X. Zhang and C. Liu. Gelcasting of complex-shaped ZrB<sub>2</sub>-SiC ultra high temperature ceramic components, *Materials Science and Engineering: A*, **556**, 2012, pp. 494-499.
- [21]. S. W. Jiang, T. Matsukawa, S. Tanaka and K. Uematsu, Effects of powder characteristics, solid loading and dispersant on bubble content in aqueous alumina slurries, *Journal of the European Ceramic Society*, **27**, 2007, pp. 879-885.
- [22]. Y. Takao, T. Hotta, K. Nakahira, M. Nakio, N. Shinohara, M. Okumiya and K. Uematsuc, Processing defects and their relevance to strength in alumina ceramics made by slip casting. *Journal of the European Ceramic Society*, **20**, 2000, pp. 389-395.
- [23]. X. Zhu, D. Jiang and S. Tan, Improvement in the strength of reticulated porous ceramics by vacuum degassing, *Materials Letters*, **51**, 2001, pp. 363-367.
- [24]. J. C. Chang, B. V. Velamakanni, F. F. Lange and D. S. Pearson, Centrifugal consolidation of Al<sub>2</sub>O<sub>3</sub> and Al<sub>2</sub>O<sub>3</sub>/ZrO<sub>2</sub> composite slurries vs interparticle potentials: particle packing and mass segregation, *Journal of the American Ceramic Society*, **74**, 1991, pp. 2201-2204.
- [25]. C. T. Wamkam1, M. K. Opoku, H. Hong and P. Smith. Effects of pH on heat transfer nanofluids containing ZrO<sub>2</sub> and TiO<sub>2</sub> nanoparticles, *Journal of Applied Physics*, **109**, 2011, pp. 024305.

- [26]. P. Bowen, Particle size distribution measurement from millimeters to nanometers and from rods to platelets, *Journal of Dispersion Science and Technology*, **23**, 2002, pp. 631-662.